ISSN 0023-1584, Kinetics and Catalysis, 2011, Vol. 52, No. 1, pp. 104–110. © Pleiades Publishing, Ltd., 2011.
Original Russian Text © L.A. Isupova, E.Yu. Gerasimov, V.I. Zaikovskii, S.V. Tsybulya, 2011, published in Kinetika i Kataliz, 2011, Vol. 52, No. 1, pp. 106–112.

Effect of the Reaction Medium on the Structure of the $La_{1-x}Ca_xMnO_3$ ($x = 0–1$) Solid Solutions Prepared by the Pechini Method

L. A. Isupova[a], E. Yu. Gerasimov[a,b], V. I. Zaikovskii[a,b], and S. V. Tsybulya[a,b]

[a] *Boreskov Institute of Catalysis, Siberian Branch, Russian Academy of Sciences, Novosibirsk, 630090 Russia*
[b] *Novosibirsk State University, Novosibirsk, 630090 Russia*
e-mail: isupova@catalysis.ru

Received April 12, 2010

Abstract—The phase composition and microstructure of $La_{1-x}Ca_xMnO_3$ ($x = 0–1$) materials prepared by the Pechini method from polymer–salt stocks were studied after testing these materials in methane oxidation. According to X-ray diffraction data, the reaction medium causes no significant changes in the samples, while high-resolution transmission electron microscopy indicates that the $x > 0.3$ samples are unstable. Under the action of the reaction medium, the perovskite structure of these samples undergoes partial decomposition accompanied by the formation of planar defects having a lower manganese content. The number and degree of segregation of these defects increase with increasing calcium content. The calcium oxide and manganese oxide phases as segregated nanoparticles are observed on the particle surface. These changes are caused by the decrease in the oxygen content of the manganites under the action of the reaction medium (T, P_{O_2}), by the formation of vacancies, and by the variation of the charge of the manganese cations, as well as by the charge ordering tendency of the manganese cations. Therefore, the observed changes in catalytic activity under the action of the reaction medium for $x > 0.3$ can be due to perovskite decomposition accompanied by the formation of planar defects, the release of the manganese oxide and calcium oxide phases, and their subsequent sintering.

DOI: 10.1134/S002315841101006X

Owing to their high thermal and chemical stability, oxides with a perovskite structure are promising materials for a variety of high-temperature applications, such as high-temperature cathodes and oxidation catalysts [1, 2]. The $La_{1-x}Ca_xMnO_3$ solid solutions possess a number of extraordinary magnetic and electronic properties, including colossal magnetoresistance and charge ordering, which make this class of oxides particularly attractive.

However, the phase composition data available from the literature for these materials are controversial. For example, it was reported that a continuous series of solid solutions forms in the system [3], that there are no solid solution for middle compositions [4], and that the range of solid solutions extends only up to $x = 0.8$. A comparative study of the $La_{1-x}Ca_xMnO_3$ oxides synthesized by ceramic and mechanochemical methods [2] led the authors to assume that the $x > 0.4$ solid solutions are possibly unstable and, as a consequence, they do not form under conditions of rapid mechanochemical synthesis.

Our in situ high-temperature X-ray diffraction study [6] of the stability of homogeneous $La_{1-x}Ca_xMnO_3$ ($x = 0, 0.5, 0.8, 1$) solid solutions synthesized by the polymer–salt (Pechini) method demonstrated that, when heated in air and in vacuo (residual pressure of ~10^{-2} Torr), these materials are stable up to 1300 and 1100°C, respectively. According to X-ray diffraction data, their composition does not change. However, a high-resolution transmission electron microscopic (HRTEM) examination of the $x = 0.8$ sample that had been heated in vacuo revealed the partial separation of the initial mixed oxide and the formation of nanosized Mn_3O_4 particles coherently bound to the main perovskite phase with a defective structure. [6]. The latter is characterized by superstructure reflections and has extended planar defects in its (101) planes. According to HRTEM data, heating of $CaMnO_3$ in vacuo generates planar defects in the $CaMnO_3$ phase and causes the partial decomposition of the perovskite phase into $CaMn_2O_4$, CaO, and Mn_3O_4 [7].

The stability of some of the oxides in the reaction medium was also indicated by our data on the catalytic activity of homogeneous solid solutions prepared by the Pechini method and calcined at 900 and 1100°C [8]. It was found that the catalytic activity of nearly all calcium-substituted samples in methane oxidation decreases during the test (T_{test} = 350–600°C). The

only exception is the $x = 0.7$ sample ($T_{calcin} = 1100°C$), which is the most active in the oxide series and retains its initial activity. The specific surface area of all oxides was higher after these tests [8]. The observed decrease in catalytic activity of the oxides under the action of the reaction medium (Fig. 1) can be caused both by the blocking of their surface by strongly bound carbonates resulting from the reaction (their effect should weaken as the test temperature is raised) and by the more profound structural changes that are due to the oxygen partial pressure being lower than in air.

Here, we report the effect of the reaction medium on the structural properties of the homogeneous $La_{1-x}Ca_xMnO_3$ solid solutions synthesized by the Pechini method.

EXPERIMENTAL

The $La_{1-x}Ca_xMnO_3$ solid solutions were synthesized in $x = 0.1$ steps by dissolving metal nitrates in water, mixing them in appropriate amounts, adding citric acid and ethylene glycol, and evaporating the solution at 70–80°C until the formation of a rubber-like polymer (polymer–salt stock). The polymer was subjected to oxidative destruction, and the resulting substance was calcined at 1100°C for 4 h.

X-ray diffraction patterns were obtained on a URD-63 diffractometer (Germany) using CuK_α radiation (2θ scan mode, 0.02° increments, counting time of 5 s per point).

HRTEM images were obtained on a JEM-2010 microscope (Japan) with 1.4 Å resolution. The elemental composition of the samples was determined by energy-dispersive X-ray (EDX) microanalysis using an EDX spectrometer with a Si(Li) detector with 130 eV energy resolution.

Catalytic activity was determined at 350–600°C using a flow reactor. Before taking measurements, the catalyst sample (particle size of 0.25–0.5 mm) was held in the reaction medium (0.9% CH_4 + 9% O_2 + 90.1% N_2, flow rate of 2.4 l/h, residence time of 1.5 s) for ~30 min. In some cases, the catalyst was held at 600°C for 1–4 h. The only oxidation products were carbon dioxide and water. The catalytic activity data were reported in our earlier publication [8].

The specific surface area was derived from thermal argon desorption data by the BET method.

Thermal analysis (TG, DTG, DTA) was performed up to 1200°C in flowing air using an STA-409 PC LUXX system (NETZSCH, Germany). The initial weight of the sample was 70 to 200 mg, and the cooling/heating rate was 10 K/min. The oxygen content was derived from the weight lost by the sample heated to 1200°C. The final composition after oxygen evolution was assumed to correspond to the manganese oxidation state Mn^{3+}, implying the formula $La_{1-x}Ca_xMnO_{3-x/2}$.

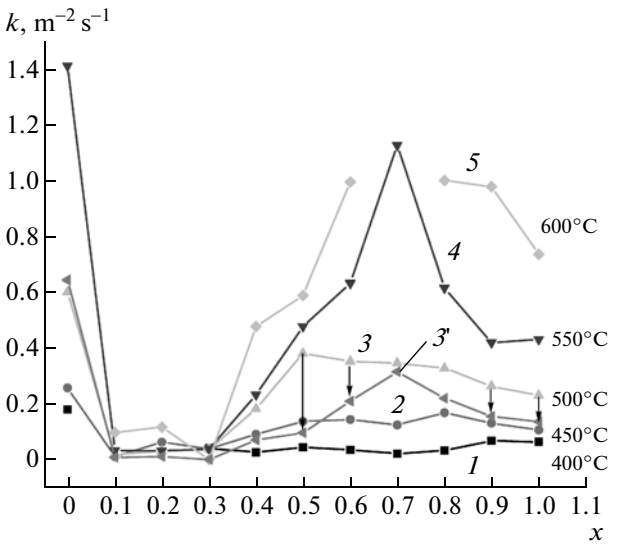

Fig. 1. Methane oxidation rate constant as a function of the calcium content (x) of $La_{1-x}Ca_xMnO_3$ [8]. The samples were calcined at 1100°C. Reaction temperature, °C: (*1*) 400, (*2*) 450, (*3, 3'*) 500, (*4*) 550, and (*5*) 600; (*3'*) sample after a catalytic test at 600°C.

RESULTS AND DISCUSSION

Phase Composition

According to X-ray diffraction data (Fig. 2), the $La_{1-x}Ca_xMnO_3$ ($x = 0.1$–0.8) solid solutions after catalytic tests in methane oxidation at 400–600°C are single-phase and have a perovskite structure (orthorhombic space group *Pnmb*). No reflections inconsistent with the *Pnmb* symmetry were observed. The $x = 0.9$–1 samples are also single-phase, but they have a monoclinic perovskite structure (space group $P2_1$). The unit cell parameters of the initial solid solution samples and of the samples subjected to catalytic tests are listed in the table, and Fig. 3 plots the unit cell volume as a function of the phase composition for the same samples. These data differ little. Note only that the catalytic tests induce a slight decrease in the unit cell volume of the $x = 0.6$–0.8 samples.

It is interesting that, in $LaMnO_3$ subjected to catalytic tests, the symmetry group is changed from orthorhombic to rhombohedral. As is known from the literature, the orthorhombic structure is typical of lanthanum manganites having a lower oxygen stoichiometry than the rhombohedral modification. Based on data reported by other authors [9, 10], we estimated the oxygen content of the unsubstituted perovskite. The unit cell parameters of the initial sample suggested the formula $LaMnO_{3.10}$, and the sample subjected to catalytic tests had a higher oxygen content corresponding to the formula $LaMnO_{3.15}$. The lower oxygen content of the fresh sample prepared by the Pechini method is likely due to the fact that, at the heat treatment stage, catalyst formation takes place under reductive conditions as a consequence of the oxida-

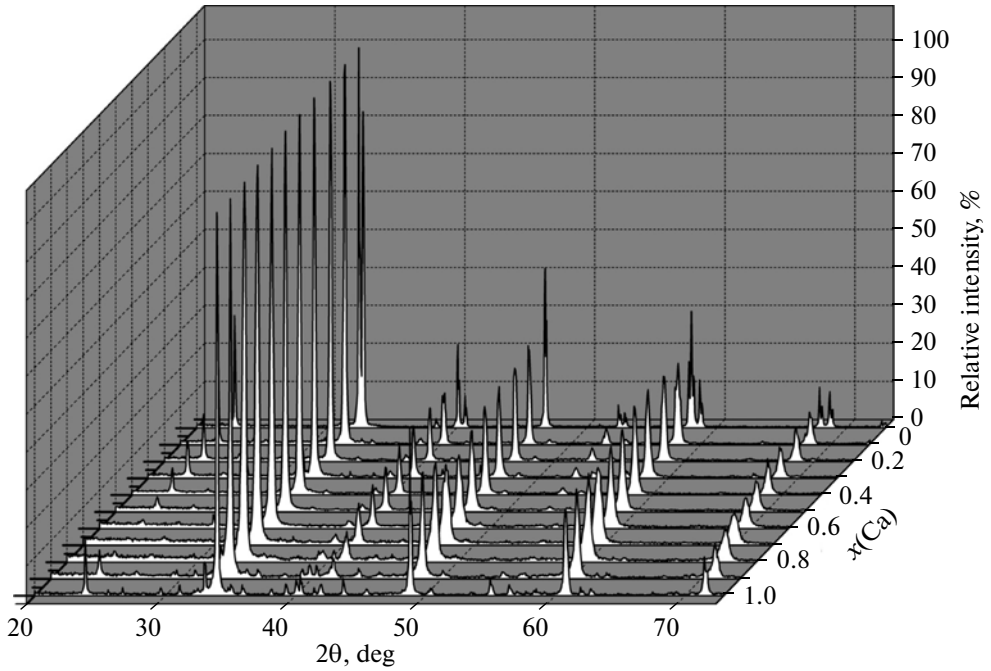

Fig. 2. X-ray diffraction patterns of the $La_{1-x}Ca_xMnO_3$ materials synthesized by the Pechini method (T_{calcin} = 1100°C, 4 h) recorded after the determination of their catalytic activity im methane oxidation at 400–600°C.

tion of the organic components of the precursor. Thus, the catalyst sample becomes more oxidized under the action of the reaction medium followed by cooling in air.

The $x = 0.5$–0.8 samples subjected to catalytic tests were assigned to orthorhombic symmetry (*Pnmb*) for the reason that their diffraction patterns showed reflections (210, 122, 221, etc.) uncharacteristic of the tetragonal space group *I*4/*mmm*, which indicated a decrease in symmetry. Apparently, the reaction medium–induced decrease in the unit cell volume observed for $x = 0.5$–0.8 (Fig. 3) is due to this decrease in symmetry. Our data indicate structural changes in these samples under the action of the reaction medium, specifically, a decrease in the symmetry of their structure, which is possibly caused by changes in their oxygen content.

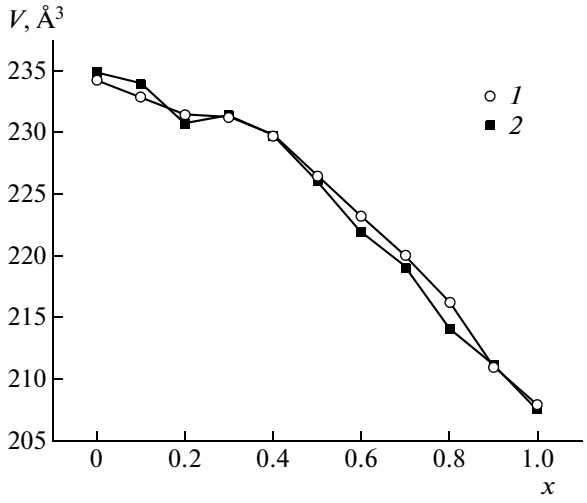

Fig. 3. Unit cell volume versus composition for $La_{1-x}Ca_xMnO_3$ (*1*) before and (*2*) after catalytic tests.

Oxygen Content from Thermoanalytical Data

The excess oxygen content of the fresh samples, determined thermoanalytically from the weight loss data for the samples heated to 1200°C in air (Fig. 4), suggest the composition $LaMnO_{3.12}$ for $x = 0$, which is close to the estimate obtained earlier from X-ray diffraction data. The introduction of calcium leads to a decrease in the oxygen content. The calculated formula of the $x = 0.1$ sample is $La_{0.9}Ca_{0.1}MnO_{3.03}$, and that of the $x = 0.7$ sample is $La_{0.3}Ca_{0.7}MnO_{2.72}$. The amount of oxygen released upon heating passes through a minimum in the series of these three samples and is 0.84, 0.58, and 0.67%, respectively. As the samples are cooled in air, their weight increases apparently because of oxygen uptake. The amount of added oxygen (0.64, 0.44, and 0.47%, respectively) is smaller than the amount of oxygen released upon heating. This can be due to the incomplete reoxidation of the samples because of kinetic limitations. Another plausible explanation is that, in the calculation of the amount of oxygen lost upon heating, we did not allow for the release of adsorbed CO_2 and H_2O, which might lead to an overestimated oxygen loss [11].

Unit cell parameters of $La_{1-x}Ca_xMnO_3$ samples before and after their testing in methane oxidation

x	Space group	a, Å	b, Å	c, Å	V, Å^3	β
			Before tests			
0	*Pnmb*	5.491(8)	5.489(9)	7.774(4)	234.31	90
0.1	*Pnmb*	5.479(3)	5.481(1)	7.758(3)	232.98	90.0
0.2	*Pnmb*	5.483(4)	5.475(2)	7.750(4)	232.65	90.0
0.3	*Pnmb*	5.475(5)	5.466(2	7.731(4)	231.36	90.0
0.4	*Pnmb*	5.458(3)	5.453(1)	7.719(4)	229.74	90.0
0.5	*I*4/*mmm*	5.430(8)	5.430(8)	7.681(8)	226.47	90.0
0.6	*I*4/*mmm*	5.406(4)	5.406(5)	7.640(7)	223.27	90.0
0.7	*I*4/*mmm*	5.380(3)	5.380(3)	7.604(6)	220.09	90.0
0.8	*I*4/*mmm*	5.350(6)	5.350(6)	7.556(5)	216.27	90.0
0.9	$P12_11$	5.298(4)	5.310(3)	7.500(5)	211.00	90.3
1	$P12_11$	5.270(3)	5.283(4)	7.466(7)	207.86	90.3
			After tests			
0	*R*3*c*/2	5.526(3)	5.526(3)	13.324(8)	234.9	90.0
0.1	*Pnmb*	5.486(5)	5.491(5)	7.764(9)	233.93	90.0
0.2	*Pnmb*	5.471(7)	5.479(8)	7.707(15)	230.75	90.0
0.3	*Pnmb*	5.463(4)	5.474(6)	7.737(5)	231.42	90.0
0.4	*Pnmb*	5.447(4)	5.463(6)	7.719(4)	229.76	90.0
0.5	*Pnmb*	5.418(3)	5.433(5)	7.679(4)	226.11	90.0
0.6	*Pnmb*	5.398(1)	5.393(1)	7.624(1)	221.97	90.0
0.7	*Pnmb*	5.365(3)	5.371(3)	7.601(2)	219.07	90.0
0.8	*Pnmb*	5.330(1)	5.328(1)	7.537(1)	214.04	90.0
0.9	$P12_11$	5.302(1)	5.309(1)	7.500(1)	211.16	89.9
1	$P12_11$	5.276(1)	5.275(2)	7.455(1)	207.53	89.9

The above data demonstrate that the oxygen content of the perovskites varies as they are heated and cooled in air. Therefore, the number of oxygen vacancies in the samples can change under the action of the reaction medium, affecting the charge of the manganese cations. This can bring about structural changes because of the tendency of the manganese cations to charge ordering and the tendency of oxygen vacancies to vacancy ordering. The role of this vacancy ordering will increase with increasing x.

Microstructure

According to HRTEM and EDX data, the catalytic tests do not change the morphology of perovskite particles in the $La_{1-x}Ca_xMnO_3$ series: 1- to 5-μm particles consisting of 0.1- to 0.5-μm microblocks remain in the samples.

Figure 5 shows the morphology and microstructure of the $LaMnO_3$ sample used in the catalytic reaction. According to HRTEM data, this sample has a rhombohedral (*R*3*c*) lattice. The particle shape and size in this sample are nearly the same as in the initial sample. Extended defects indicative of changes in microstructure are not observed either.

Starting at $x = 0.3$, the samples subjected to catalytic tests, as distinct from their fresh counterparts, have multiple planar defects, and these defects build up as with increasing x. Starting at $x = 0.5$, the oxides CaO and Mn_3O_4 are detected in the samples along with the planar defects. The size of a manganese oxide particle is ~100 nm. It is interesting that these particles

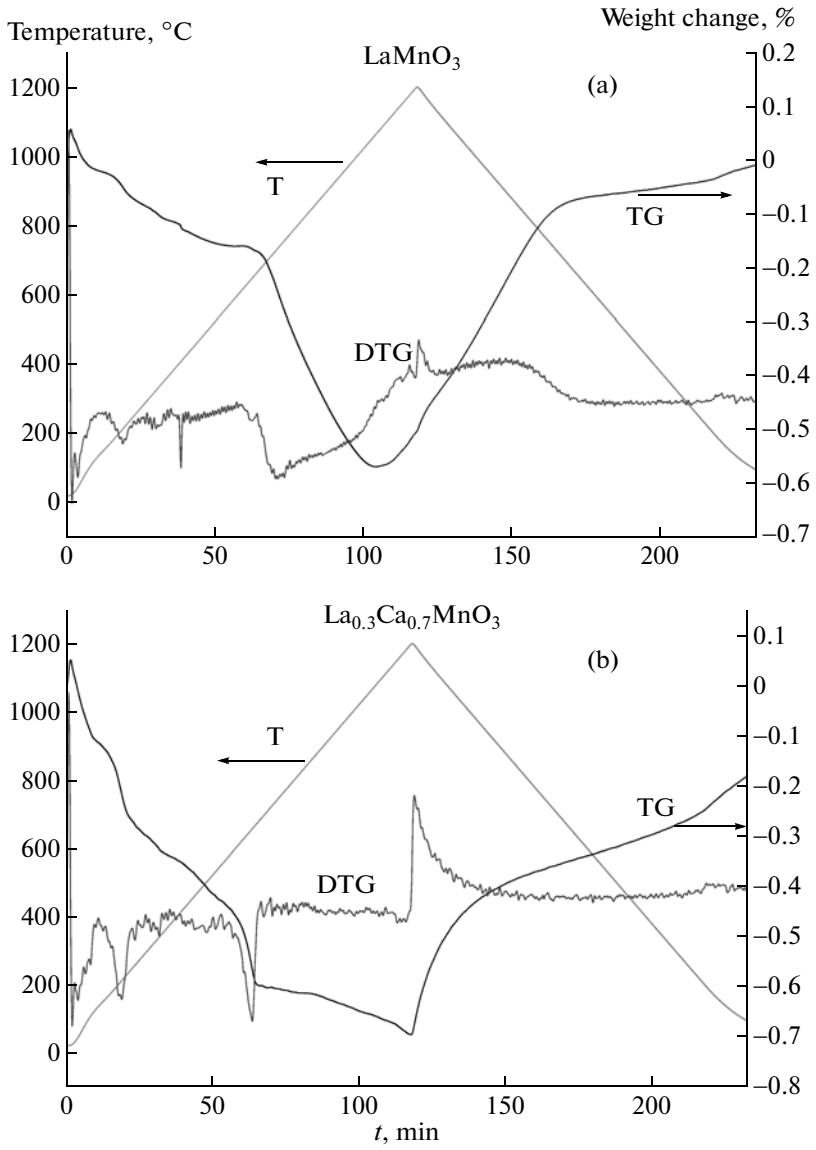

Fig. 4. Thermoanalytical data obtained in the heating and cooling modes for (a) $LaMnO_3$ and (b) $La_{0.3}Ca_{0.7}MnO_3$.

consist of microblocks 10 to 20 nm in size. Figure 6 shows the microstructure of the $x = 0.7$ sample. It can be seen that planar defects have formed and segregated along the (001) planes.

In the calcium-rich sample with $x = 0.9$, the planar defects segregate to form an ordered structure with the quadruple perovskite lattice constant along the [001] direction (Fig. 7). According to EDX data, the given area has a substoichiometric Mn content. The deficit of Mn cations is 20% of the normal cationic stoichiometry. It is likely that these regions are responsible for the formation of nanosized (10–20 nm) Mn_3O_4 particles (as in the vacuum-treated samples; see Fig. 8 [6]) followed by the sintering of these particles into blocks (100 nm).

The above data demonstrate the instability of the $x > 0.3$ samples in the reaction medium. Apparently, the thermal evolution of oxygen from the calcium-rich samples causes the segregation of the resulting oxygen vacancies, which is accompanied by the formation of multiple planar defects in the perovskite structure and causes the decrease in the symmetry of the structure. It is not impossible that the changes in the oxygen content of the perovskites under the action of the reaction medium and the corresponding changes in the charge of the manganese cations (according to the electroneutrality principle) obey the manganese cation charge ordering regularities considered by Lebedev et al. [12]. These changes cause partial perovskite decomposition yielding nanosized manganese oxide

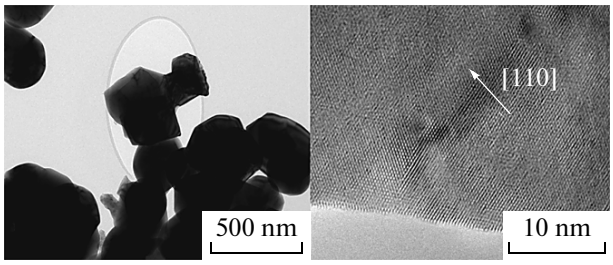

Fig. 5. HRTEM image of $LaMnO_3$ after the catalytic reaction.

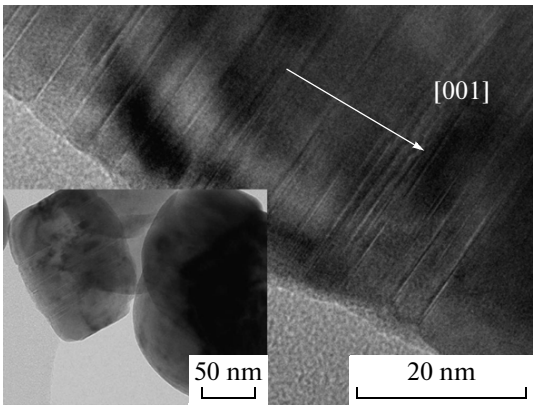

Fig. 6. HRTEM image of $La_{0.3}Ca_{0.7}MnO_3$ after the catalytic reaction.

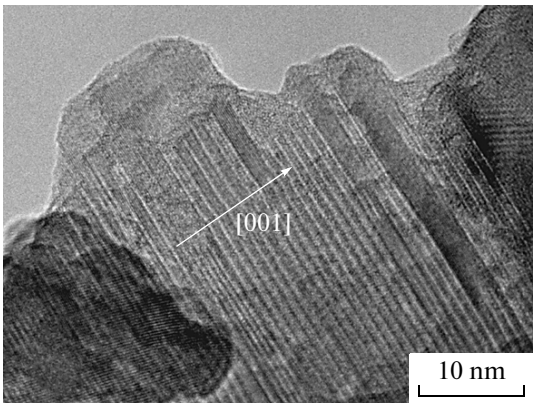

Fig. 7. HRTEM image of $La_{0.1}Ca_{0.9}MnO_3$ after the catalytic reaction.

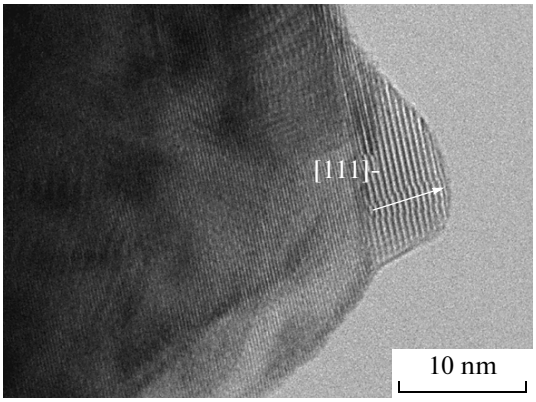

Fig. 8. HRTEM image of $La_{0.2}Ca_{0.8}MnO_3$ neat-treated in vacuo: a γ-Mn_3O_4 particle epitaxially bound to perovskite [6].

and calcium oxide particles, which then segregate under the action of the reaction medium to form larger, microblock particles. Apparently, the planar defects forming in the reaction medium (which is poorer in oxygen than air) persist as the sample is cooled in air and are, therefore, observable. At the same time, at low calcium contents ($x < 0.3$), the planar defects do not form under the reaction conditions and the resulting point defects reoxidize as the sample is cooled in air. The results of this study indicate the partial decomposition of the $x > 0.3$ perovskites under the action of the reaction medium and the formation of calcium oxide and manganese oxide particles on their surface. The absence of reflections from these phases in the X-ray diffraction patterns can be due to the small size (<10 nm) of the microblocks constituting the oxide particles or the low percentage of these phases (<5%).

The comparative study of the microstructures of the $x = 0.5–1$ samples before and after methane oxidation demonstrated that the reaction medium induces the formation of planar defects and nanosized Mn_3O_4 particles in the perovskites, whose degree of segregation was found to increase with increasing x. Therefore, the increase in the catalytic activity of the perovskites that was observed as x was raised from 0.3 to 0.7 [8] can be due to the increasing proportion of released manganese oxide and the still weak segregation of planar defects in the perovskite structure (which ensures the high reactivity of the perovskite). The decrease in catalytic activity for $x > 0.7$ accompanied by a further buildup of released manganese oxide is caused either by the segregation of manganese oxide particles and planar defects (which reduces the reactivity of the perovskite) or by the change in the perovskite structure. Accordingly, the observed deactivation of the perovskites under the action of the reaction medium [8] can be due not only to the formation of surface carbonates [13] (as was hypothesized earlier), bust also to the aggregation of the primary nanosized particles of manganese oxide into larger particle blocks and defect ordering in the perovskite structure (Fig. 9).

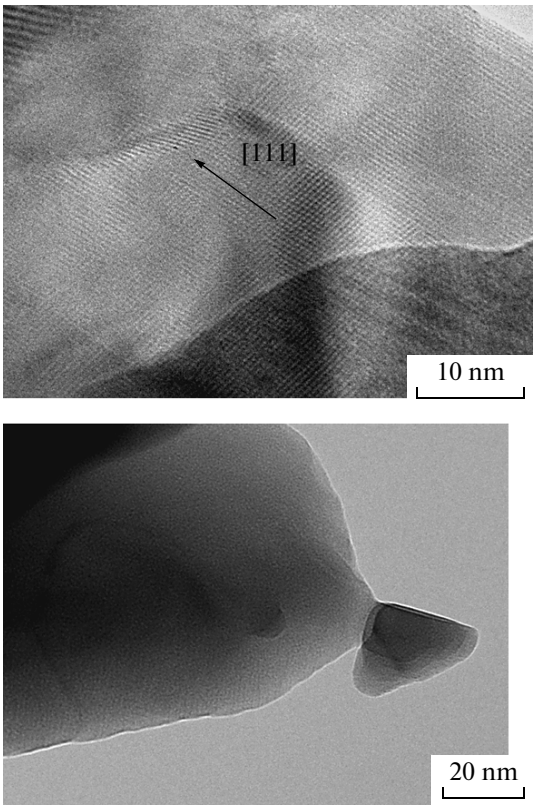

Fig. 9. HRTEM images of $La_{0.3}Ca_{0.7}MnO_3$ after the reaction, showing large Mn_3O_4 blocks.

CONCLUSIONS

The investigation of the effect of the reaction medium on the properties of the substituted manganites synthesized by the Pechini method demonstrated that, although X-ray diffraction did not reveal any changes in the phase composition of the perovskites, the $x > 0.3$ samples are unstable, according to HRTEM data. The reaction medium induces partial decomposition of the perovskite phase, which is accompanied by the formation of planar defects (having a lower manganese content) in the structure of this phase, whose number and degree of segregation increase with an increasing proportion of calcium, and by the appearance of calcium and manganese oxides as segregated nanoparticles on the surface. Evidently, these changes are brought about by the variation of the oxygen content of the perovskite (similar structural changes were observed by us in samples heated at a low oxygen partial pressure) and the corresponding changes in the charge of the manganese cations, as well as by the charge ordering tendency inherent in manganese cations. Therefore, the initial activity of the $x > 0.3$ samples in the reaction medium can be due to the above-described perovskite decomposition and the release of manganese oxide nanoparticles on the surface. The monotonic decline of catalytic activity during the reaction might arise from the subsequent segregation of these particles ad from defect ordering in the perovskite structure, specifically, the formation and segregation of planar defects. Since both the number of planar defects and their degree of segregation vary in the perovskites, this can affect the state of active sites on the surface. It is possible that the higher activity and stability of the $x = 0.7$ sample, as compared to the $x > 0.7$ samples, in the reaction medium observed against the background of perovskite breakdown and the sintering of the resulting oxides, are due to the larger proportion of manganese oxide on the surface and the lower degree of segregation of the planar defects. However, this issue needs further investigation.

ACKNOWLEDGMENTS

This work was supported by the Ministry of Education and Science of the Russian Federation through the program "Development of the Scientific Potential of the Higher Education Institutions" (grant no. 2.1.1/729).

REFERENCES

1. Izyumov, Yu.A. and Skryabin, Yu.N., *Usp. Fiz. Nauk*, 2001, vol. 171, no. 2, p. 121 [*Phys.-Usp.* (Engl. Transl.), vol. 171, no. 2, p. 109].
2. Isupova, L.A., Tsybulya, S.V., Kryukova, G.N., Alikina, G.M., Boldyreva, N.N., Yakovleva, I.S., Ivanov, V.P., and Sadykov, V.A., *Solid State Ionics*, 2001, vols. 141–142, p. 417.
3. Rormark, L., Wiil, K., Stolen, S., and Grande, T., *J. Mater. Chem.*, 2002, vol. 12, p. 1058.
4. Majewski, P.L., Epple, L., Rozumek, M., Schluckwerder, H., and Aldinger, F., *J. Mater. Res.*, 2000, vol. 5, p. 1161.
5. Slobodin, B.V., Surat, L.L., and Vladimirova, E.V., *J. Alloys Compd.*, 2002, vol. 335, p. 115.
6. Gerasimov, E.Yu., Zaikovskii, V.I., Tsybulya, S.V., and Isupova, L.A., *Poverkhnost*, 2009, no. 10, p. 10.
7. Gerasimov, E.Yu., Zaikovskii, V.I., Isupova, L.A., and Tsybulya, S.V., *Vestn. Novosib. Gos. Univ., Ser. Fiz.*, 2009, vol. 4, no. 4, p. 59.
8. Isupova, L.A., Gerasimov, E.Yu., Zaikovskii, V.I., Tsybulya, S.V., Kulikovskaya, N.A., and Saputina, N.F., *Kinet. Katal.*, 2009, vol. 50, no. 6, p. 922 [*Kinet. Catal.* (Engl. Transl.), vol. 50, no. 6, p. 886].
9. Barnabe, A., Gaudon, M., Bernard, C., Laberty, C., and Durand, B., *Mater. Res. Bull.*, 2004, vol. 39, p. 725.
10. Sakai, N., Fjellvag, H., and Lebech, B., *Acta Chem. Scand.,* 1997, vol. 51, p. 904.
11. Nadev, A.N., Tsybulya, S.V., Belyaev, V.D., Yakovleva, I.S., and Isupova, L.A., *Zh. Strukt. Khim.*, 2008, vol. 49, no. 6, p. 1115.
12. Lebedev, O.I., van Tendeloo, G., Amelinckx, S., Leibold, B., and Habermeier, H.-U., *Phys. Rev. B: Condens. Matter*, 1998, vol. 58, no. 12, p. 8065.
13. Krylov, O.V., *Geterogennyi kataliz: Uchebnoe posobie* (Heterogeneous Catalysis: A Textbook), Novosibirsk: Novosib. Gos. Univ., 2002, vol. 3, p. 61.